Optogenetic manipulation of medullary neurons in the locust optic lobe

Hongxia Wang[1], Richard B. Dewell[1], Markus U. Ehrengruber[2], Eran Segev[3], Jacob Reimer[1], Michael L. Roukes[3], Fabrizio Gabbiani[1,4,*]

[1]Department of Neuroscience, Baylor College of Medicine, Houston, TX,
[2]Department of Biology, Kantonsschule Hohe Promenade, Zurich, Switzerland,
[3]Department of Applied Physics and Material Science, California Institute of Technology, Pasadena, CA,
[4]Electrical and Computer Engineering Department, Rice University, Houston, TX

Running Head

Optogenetics in locusts

Address for correspondence

Fabrizio Gabbiani,
Baylor College of Medicine,
Department of Neuroscience,
One Baylor Plaza, Houston, TX, 77030.
Email: gabbiani@bcm.edu
Phone: (713)-798-1849.

Authors' contributions

H.W., M.U.E., J.R., M.L.R. and F.G. designed the experiments; E.S. fabricated the laser probe; H.W. performed the experiments with the assistance of R.B.D and J.R.; H.W. carried out the data analysis with the assistance of R.B.D.; H.W. and F.G. co-wrote the paper.

Abstract

Locust is a widely used animal model for studying sensory processing and its relation to behavior. Due to the lack of genomic information, genetic tools to manipulate neural

circuits in locusts are not yet available. We examined whether Semliki Forest virus is suitable to mediate exogenous gene expression in neurons of the locust optic lobe. We subcloned a channelrhodopsin variant and the yellow fluorescent protein Venus into a Semliki Forest virus vector and injected the virus into the optic lobe of locusts (*Schistocerca americana*). Fluorescence was observed in all injected optic lobes. Most neurons that expressed the recombinant proteins were located in the first two neuropils of the optic lobe, the lamina and medulla. Extracellular recordings demonstrated that laser illumination increased the firing rate of medullary neurons expressing channelrhodopsin. The optogenetic activation of the medullary neurons also triggered firing of a postsynaptic, looming-sensitive neuron, the Lobula Giant Movement Detector (LGMD). These results indicate that Semliki Forest virus is efficient at mediating transient exogenous gene expression and provides a tool to manipulate neural circuits in the locust nervous system and likely other insects.

New and Noteworthy

Using Semliki Forest virus, we efficiently delivered channelrhodopsin into neurons of the locust optic lobe. We demonstrate that laser illumination increases the firing of the medullary neurons expressing channelrhodopsin and of an identified postsynaptic target neuron, the LGMD neuron. This technique allows to manipulate the neuronal activity in locust neural circuits using optogenetics.

Keywords

Locust, optogenetics, medulla, LGMD, Semliki Forest virus

Introduction

Insects are widely used to address fundamental questions about brain mechanisms. Research on insects has broadened our knowledge and helped us understand the neural basis of complex behavior, e.g., communication and navigation in bees and ants (Evangelista et al., 2014; Srinivasan, 2010; Wehner, 2003), vision and motion detection in flies (Egelhaaf, 2008), olfactory learning and odor discrimination in flies, sphinx moths and locusts (Gupta and Stopfer, 2011), auditory processing in crickets (Göpfert and Hennig, 2016), as well as the mechanisms of neural development and genetics, most recently mainly in *Drosophila* (Hales et al., 2015; Spindler and Hartenstein, 2010). In these endeavors, genetic tools are helpful for dissecting neural circuits and deciphering the neural mechanisms underlying different behaviors. The Gal4-UAS system, for instance, is one of the most powerful ways of achieving targeted gene expression in *Drosophila* that has been adapted to other model systems (Asakawa and Kawakami, 2008; Brand and Perrimon, 1993; Busson and Pret, 2007; Imamura et al., 2003). This binary system is widely used to create transgenic flies by combining a driver (Gal4) and responder (UAS) line based on the properties of the yeast transcription factor GAL4 which activates its target genes by binding to UAS *cis*-regulatory sites. Since most neurons in *Drosophila* are small, they are unsuitable for intracellular dendritic recordings, making this model system of limited use for investigations of dendritic computations in single cells. On the other hand, insects with larger neurons such as locusts, crickets or moths have proven optimal for intracellular electrophysiological recordings. In most of these insects, however, it is not easy to manipulate gene expression and carry out genome editing due to lack of genome sequencing information and long generation times. Nevertheless, researchers have developed a variety of genetic tools for several such species. For example, *piggyBac*-derived cassettes have been integrated in the honeybee (*Apis mellifera*) expressing the fluorescent markers Rubia and EGFP under either an artificial or an endogenous promoter (Schulte et al., 2014). In another case, an odorant receptor co-receptor (orco) mutated ant germ line has been generated in *Ooceraea biroi* using CRISPR/Cas gene editing technology (Trible et al., 2017).

Locust is a popular model for studying behavior relying on visual motion, especially

87 visually-evoked escape and collision-avoidance behavior (Fotowat and Gabbiani, 2011).
88 Creating transgenic locust germ lines or developing an efficient neuronal transfection
89 method in locusts would be desirable to increase the power of this model system.
90 However, up to now, there are no known reports on any foreign transformation in the
91 nervous system of locusts. Optogenetics is an efficient stimulation method to control
92 neuronal activity using light-gated ion channels, such as channelrhodopsin,
93 halorhodopsin and their variants (Arrenberg et al., 2009; Boyden et al., 2005; Ishizuka et
94 al., 2006). It has been broadly used to map neural circuitry, study neuronal activity,
95 control cardiac function, and treat photoreceptor degeneration and Parkinson disease
96 (Adamantidis et al., 2007; Arenkiel et al., 2007; Bi et al., 2006; Gradinaru et al., 2009).
97
98 Semliki Forest virus (SFV) is an enveloped single-stranded, positive RNA virus, one of
99 the members in the alphavirus family (Strauss and Strauss, 1994). In earlier work, wild-
100 type SFV and mutant SFV A7(74) were used to drive LacZ and GFP expressions in
101 pyramidal neurons of cultured hippocampal slices (Ehrengruber et al., 1999, 2003).
102 Similarly, the less cytopathic mutant SFV(PD) (Lundstrom et al., 2003) drove protein
103 expression in the rat calyx of Held *in vivo* (Wimmer et al., 2004). Since SFV is a
104 mosquito-borne pathogen, it could possibly infect other non-host insect cells (Lwande et
105 al., 2013), as has been shown for the Sindbis virus (Lewis et al., 1999). To test the
106 possibility that SFV could drive foreign gene expression in locust neurons, we inserted
107 into a SFV A7(74) based vector (Ehrengruber et al., 2003) the channelrhosopin variant,
108 Chop-Wide Receiver (ChopWR), tagged with a fluorescent marker, Venus (Wang et al.,
109 2009) and downstream of a strong ubiquitous promoter. ChopWR is a chimeric protein of
110 Chop1 and Chop2 (Nagel et al., 2003), mediating a larger photocurrent (Wang et al.,
111 2009). This plasmid was electroporated into baby hamster kidney 21 (BHK) cells for
112 generating the virus, which was injected through the eye into the optic lobe of locusts.
113
114 In this paper, we show that viral replicons based on the SFV A7(74) strain successfully
115 express ChopWR-Venus in medullary neurons of the locust optic lobe, enabling us to
116 manipulate optogenetically the activity of medullary neurons and of the LGMD, a
117 downstream neuron which plays a vital role in collision avoidance behavior (Fotowat and

118 Gabbiani, 2011).

119

120 Materials and Methods

121

122 Generation of Semliki Forest virus with ChopWR-Venus and injection in locusts

123 The generation of SFV vectors was described in previous papers (e.g., Ehrengruber et al.,
124 2011). Briefly, the ChopWR-Venus gene was first subcloned into the pENTR2B entry
125 vector and then transferred to the pScaA7-RFA destination vector by using the attB1 and
126 attB2 attachment sites through Gateway Technology (Thermo Fisher Scientific,
127 Waltham, MA). The destination vector pScaA7-RFA was obtained from a modified SFV
128 A7(74) vector plasmid, pSFV(A774nsP) (Ehrengruber et al., 2003), by moving
129 A7(74)nsP1-4 into the pSCA plasmid (DiCiommo and Bremner, 1998). This plasmid
130 uses the CMV/T7 promoters instead of the SP6 promoter and is compatible with Gateway
131 Technology. The plasmid map of the pScaA7-RFA vector containing ChopWR-Venus is
132 illustrated in Fig. 1A. The ChopWR-Venus gene was inserted downstream of the
133 endogenous SFV subgenomic promoter that follows the sequence of SFV non-structural
134 protein 4 (nsP4). Unique restriction sites are indicated in Fig. 1A, as is the simian virus
135 40 polyadenylation (SV40 polyA) terminator sequence, the Ampicillin resistance gene,
136 and the pBR322 origin of replication. The resulting plasmid and the auxiliary plasmid
137 pSFV-helper2 were purified and linearized with the restriction enzyme Spe I (New
138 England Biolabs, Ipswich, MA; NEB). The pENTR2B and pScaA7 plasmids were a gift
139 from Dr. Keith Murai (McGill University) and the pSFV-helper2 plasmid was a gift of
140 Dr. Alan L. Goldin (University of California, Irvine). T7 and Sp6 RNA polymerase
141 (Thermo Fisher Scientific) were used to catalyze the formation of RNAs from linearized
142 pScaA7-ChopWR-Venus and pSFV-helper2 DNAs, respectively. To produce viruses, *in*
143 *vitro* transcribed RNA from pScaA7-ChopWR-Venus and pSFV-Helper2 were co-
144 electroporated into BHK-21 cells. After that, BHK-21 cells were incubated for 24-48 h in
145 minimum essential (α-MEM) medium containing 5% fetal bovine serum (FBS) at 31 °C
146 with 5% CO_2 (Thermo Fisher Scientific, Waltham, MA). The SFV replicons were
147 harvested and activated by 500 μg/ml α-chymotrypsin for 30 minutes at room
148 temperature, and the reaction was stopped by 250 μg/ml aprotinin (Sigma-Aldrich, St.

149 Louis, MO). The SFV virus titers were ~1×10^5 infectious particles per ml. Experiments
150 were done using both male and female locusts, *Schistocera americana*, 8-10 weeks old.
151 The locusts were fed with grass sprayed with a solution containing *all-trans*-retinal (1
152 mM, Toronto Research Chemicals, North York, ON, Canada) for 2 days before being
153 injected with ~1-2 μl of viral solution into the right eye using a glass pipette under a
154 Leica stereomicroscope. All protocols were approved by the Bio-Environmental Safety
155 Committee of Baylor College of Medicine.
156
157 **Pilot experiments with other virus expression systems**
158 In preliminary experiments, we tested several additional viral delivery vectors. Sindbis
159 virus with the SP6 promoter was prepared similarly as described above. The titer for
160 Sindbis virus was 5×10^6 infectious particles per ml. Recombinant, GFP-tagged
161 baculovirus with the polyhedrin promoter was purchased from a commercial supplier
162 (#C14, AB Vector; titer: 10^8 pfu/ml). Recombinant adeno-associated virus (AAV)-eGFP
163 with the CMV promoter was a gift from Dr. Matthew Rasband (Baylor College of
164 Medicine; titer: 1×10^{13} GC/ml). In each case, 1-2 μl of solution containing each virus was
165 injected into the locust right eye using a glass pipette under a Leica stereomicroscope.
166 Other procedures were as for the SFV vector.
167
168 **Electrophysiology**
169 The dissection of the locust optic lobe was described in previous papers (e.g., Gabbiani et
170 al., 2002). The LGMD was stained with Alexa 594 by intracellular negative current pulse
171 injection. The Venus-tagged presynaptic neurons, especially their axon terminals, and the
172 LGMD were visualized using two-photon microscopy. The excitation wavelength was set
173 at 830 nm for Alexa 594 and 920 nm for Venus. Sharp electrodes (~10-20 MΩ) were
174 used for intracellular recording from the LGMD. Initially, spikes of the descending
175 contralateral movement detector (DCMD) neuron were recorded extracellularly by
176 positioning hook electrodes around the ventral nerve cord. DCMD spikes allowed us to
177 identify the LGMD in the lobula since they are in one-to-one correspondence with
178 LGMD spikes (O'Shea and Williams, 1974). A 488 nm Cyan Laser (Newport, Model No.
179 PC13589, Ottawa, ON, Canada) with maximum output of 20 mW was used to stimulate

180 ChopWR-expressing neurons in the optic lobe. Medullary neuronal activity was recorded
181 by using a pair of 5 MΩ tungsten electrodes (FHC, Bowdoin, ME; see Wang et al., 2018
182 for details).
183
184 **Optogenetic stimulation**
185 Optic fibers (Thorlabs, Newton, NJ) with diameters of 10, 25 and 200 μm were used to
186 deliver laser light. The optic fiber was connected to the 488 nm Cyan laser via a
187 collimator (F240FC-A, Thorlabs). The area of the incident laser beam arriving at the
188 optic lobe was ~1 mm^2. The laser power was varied between 2 and 20 mW by inserting
189 neutral density filters at the output port of the laser, immediately prior to the collimator,
190 with transmission rates of 10%, 25%, 40%, 63% and 79%, respectively. To restrict the
191 number of activated neurons, a custom-designed laser probe yielding a laser beam with a
192 diameter of ~10 μm was used in a subset of experiments (Segev et al., 2016). The time
193 interval between two successive laser stimulations was 2 minutes to minimize
194 desensitization of the responses. To minimize photoreceptor activation from reflected
195 laser light, the eye was covered with black wax and/or black vinyl tape during laser
196 stimulation. Despite this precaution, light hitting the back of the eye caused small,
197 transient photoreceptor activations when the laser switched on and off.
198
199 **Injection of picrotoxin in the lobula**
200 To investigate whether inhibitory neurons presynaptic to the LGMD had been activated
201 by the laser stimulation, picrotoxin (5 mM; Sigma-Aldrich) dissolved in water was puffed
202 along the dorsal edge of the lobula, close to the region where the inhibitory dendrites of
203 the LGMD's field C arborize. The injected solution contained 0.5 % of the colorant fast
204 green (Sigma-Aldrich) to visualize the tip of the injection pipette and the amount of
205 solution injected in the lobula. The injection pipette's tip diameter varied between 1 and
206 2.5 μm. After injection, the dye diffused around the injection site and stayed confined to
207 the lobula. A picospritzer was used to control the duration and puffing pressure (8 psi/55
208 kPa; WPI, Sarasota, FL). Based on earlier work (Dewell and Gabbiani, 2018), the
209 estimated final concentration of drug at the level of field C was ≤ 200 μM.
210

211 **Data analysis and statistics**

212 Custom Matlab (The MathWorks, Natick, MA) code was used for data analysis. The raw
213 data recorded from medullary neurons were first normalized; the spikes were then
214 detected with a set threshold (see Wang et al., 2018, for details). Spikes within 1.5 ms of
215 a previously detected spike were excluded. To calculate instantaneous firing rates (IFRs)
216 during looming stimuli, the spike train of the LGMD and the medullary neurons were
217 convolved with a Gaussian filter that had a standard deviation of 20 ms. In Fig. 2E, the
218 membrane potential (V_m) of the LGMD was median filtered over a time window of 25 ms
219 to eliminate spikes and reveal the subthreshold V_m time course. For the same reason, in
220 Fig. 2F the average LGMD's V_m during laser stimulation was calculated as its median
221 value during the time interval when the laser was turned on. It was compared with the
222 LGMD's V_m during spontaneous activity, calculated as the median value during the time
223 interval from the start of recording to the start of laser stimulation (>1 s). Medians for
224 each trial where then averaged across 3-5 trials per animal. When using the custom laser
225 probe no spiking was evoked and the LGMD's V_m during laser stimulation was
226 calculated as the mean of V_m during the time when the laser was turned on (Fig. 5B). It
227 was compared with the LGMD's V_m during spontaneous activity, calculated as the mean
228 within 1 s before the start of laser stimulation (Fig. 5C).

229

230 The one-sided Wilcoxon signed-rank test (WSRT) was used to compare the statistical
231 differences between groups of spontaneous activities and activities stimulated by
232 optogenetics with or without picrotoxin treatment. All the data are described as mean ±
233 s.d. (standard deviation).

234

235 ## Results

236

237 **Semliki Forest Virus drives expression of ChopWR-Venus in locust medullary**
238 **neurons**

239 In pilot experiments, we tested with little success the capacity of several viruses to
240 transfect locust optic lobes neurons, including adeno-associated virus (AAV), Sindbis and
241 baculovirus. Although AAV is not known to infect arthropods, other members of its

242 family, as well as Sindbis and baculovirus do (Cotmore et al., 2014; Lewis et al., 1999;
243 Oppenheimer et al., 1999). In contrast, three days after recombinant SFV injection,
244 ChopWR-Venus was observed expressing on the membrane of medullary neurons cell
245 bodies, axonal fibers, and presynaptic terminals in the lobula (Fig. 1B, a-d). When the
246 LGMD was concurrently stained with the fluorescent dye Alexa 594, some axon
247 terminals overlapped with the dendritic branches of the LGMD (Fig. 1B, c, d).
248 Additionally, stained neurons were also observed in the lamina in some experiments,
249 when viral solution was deposited there upon retraction of the injection pipette (not
250 shown). These results indicate that the SFV A7(74) plasmid vector can efficiently deliver
251 a gene of interest into neurons of the medulla (and lamina) of the locust optic lobe. Five
252 of 70 animals injected with virus died; all other locusts were healthy and did not appear
253 to be affected negatively by the manipulation during the experiments.
254
255 **Optogenetic stimulation of medullary neurons activates the LGMD**
256 As demonstrated in Fig. 2A, the instantaneous firing rate (IFR) of transfected medullary
257 neurons increased in response to a 5 s long laser pulse. On average, the spontaneous
258 firing rate of medullary units recorded from a pair of tungsten electrodes was 19.4 ± 12.2
259 spk/s (mean ± s.d.), while optogenetics stimulation increased the rate to 48.9 ± 20.0 spk/s
260 (Fig. 2B). The IFR of the LGMD increased as well (Fig. 2C). On average, the mean firing
261 rate of the LGMD in response to laser stimulation increased from 0 to 7.9 ± 5.1 spk/s
262 (Fig. 2D). The turning ON and OFF of the laser caused brief spike bursts in the medullary
263 neurons (Fig. 2A, arrowheads). Correspondingly, the LGMD fired an initial spike right
264 after the ON transition (Fig. 2C, arrowhead) which was immediately followed by a
265 transient membrane potential (V_m) hyperpolarization of ~1 s duration, also observed right
266 after the laser was turned OFF (Fig. 2E top, arrowheads). During the laser stimulation,
267 the LGMD V_m was depolarized by 3.8 ± 3.0 mV (Fig. 2E, F) in the ChopWR expressing
268 locusts. In uninjected controls, transient responses occurred with laser onset and offset,
269 but no sustained membrane potential depolarization was observed (Fig. 2E bottom).
270 These results imply that optogenetic manipulation of medullary neurons is able to
271 modulate the activity of one downstream target neuron, the LGMD.
272

273 **Block of inhibition enhances LGMD firing to optogenetic stimulation**

274 To isolate the excitatory inputs to the LGMD, the $GABA_A$ receptor antagonist, picrotoxin
275 was puffed at the dorsal edge of the lobula, where inhibitory dendritic branches of the
276 LGMD are located. Compared with the control group, block of inhibition increased the
277 firing of the LGMD in response to the laser stimulation (Fig. 3A and B). The LGMD
278 firing rate caused by the laser stimulation increased from 1.8 ± 0.8 to 7.9 ± 4.3 spk/s after
279 adding picrotoxin (Fig. 3C). Addition of picrotoxin removed the hyperpolarizations
280 observed at the onset and offset of the laser pulse (Fig. 2E), and instead the luminance
281 change caused by the laser turning on and off produced transient bursts with peak firing
282 rates of 69.9 ± 75.1 and 48.8 ± 48.2 spk/s after $GABA_A$ blockade (Fig. 3B, D and E).
283 These results demonstrate that the combination of blocker and optogenetic stimulation
284 was effective at isolating the excitatory input to the LGMD.

285

286 **Laser power affects the firing of the LGMD**

287 Next, we tested whether optogenetic activation of the LGMD depends on the strength of
288 the laser power stimulus used to activate channelrhodopsin. As demonstrated for one
289 example in Fig. 4A, the mean number of spikes of the LGMD across 5 trials increased
290 from 19.8 ± 3.3 to 44.6 ± 14.7 when power increased from 2 to 8 mW. However, at the
291 higher power of 16 mW, the number of LGMD spikes elicited by the laser stimulus was
292 slightly lower, 33.2 ± 11.9. We further investigated the effect of laser power in 5 animals
293 by using 6 values varying from 2 to 20 mW (Fig. 4B). As shown in Fig. 4B, we found
294 that spiking increased when power was increased from 2 to 5 and 8 mW (18.4 ± 6.2, 31.3
295 ± 19.1 and 37.7 ± 23.3, respectively). However, higher powers of 13, 16 and 20 mW
296 resulted in slightly decreased spiking output than at 8 mW (28.2 ± 19.0, 28.4 ± 16.9 and
297 30.6 ± 17.4, respectively). The decrement might be caused by desensitization of channel
298 rhodopsin at stronger laser power (Lin, 2011; Wang et al., 2009). These results indicate
299 that optogenetic activation of the LGMD can be modulated by the laser power strength
300 for a given expression level of Chop-WR in medullary neurons.

301

302 **Narrow laser beam produces less LGMD activation**

303 When we varied the diameter of the optic fibers used to deliver the stimulus to the optic
304 lobe from 10 to 200 μm we found that the illuminated region did not change much,
305 always being ~1 mm^2. To further spatially restrict the number of neurons activated by the
306 laser stimulus, we replaced the optic fiber with a specialized custom laser probe with an
307 exit beam diameter of 10 μm (Fig. 5A; Methods). As demonstrated in Fig. 5B,
308 illumination transmitted by this laser probe triggered EPSPs but no spiking in the LGMD,
309 except for the spikes evoked by the on and off stimulation caused by the laser light onset
310 and offset. The average LGMD's V_m during laser probe illumination was significantly
311 depolarized 0.5 ± 0.3 mV and 0.2 ± 0.3 mV in the first 2 s and over the whole duration of
312 laser illumination. These results indicate that the modified laser probe is suitable for
313 restricting the number of neurons activated by laser light.
314

315 **Discussion**

316

317 In this study, we demonstrated that SFV A7(74) drove ChopWR-Venus expression on the
318 cell membrane of medullary neurons in the locust optic lobe. Laser illumination increased
319 the firing rate of the medullary neurons expressing ChopWR-Venus and triggered the
320 firing of a downstream lobula neuron, the LGMD, which plays a key role in the locust
321 visual collision-detection circuit. SFV A7(74) mediated highly efficient expression of
322 ChopWR-Venus and led to the labelling of many neurons in the region surrounding the
323 injection site. These findings provide a way to express genes of interest in locust neurons
324 and to modulate neuronal activity using optogenetics. Besides optogenetics, GCaMP
325 calcium indicators (Akerboom et al., 2012) are future candidates for expression in locust
326 medullary neurons via SFV A7(74) transfection. These tools will help identify
327 anatomically medullary neurons and study their roles in specific visual processing tasks
328 through characterization of their calcium responses to different visual stimuli.
329

330 The responses immediately after the laser onset and offsets (arrowheads in Fig. 2; initial
331 spikes in Figs. 3 and 4) were likely caused, in part, by photoreceptor activation from
332 scattered laser light hitting the back of the eye. In experiments without viral transfection,
333 no prolonged change in LGMD activity occurred in response to laser stimulation (Fig.

334 2E, bottom). The prolonged activation of medullary neurons and the LGMD during laser
335 illumination were not attributable to the activation of photoreceptors, and therefore are
336 believed to be solely due to the light-gated ChopWR current influx into the medullary
337 neurons.
338
339 Because the large number of medullary neurons expressing ChopWR-Venus contained a
340 mixture of both excitatory and inhibitory neurons, it was hard to precisely control
341 neuronal activation of the LGMD through optogenetic stimulation. Reducing the area of
342 laser illumination is one way to get more specific activation. We tested a specialized
343 custom laser probe that minimizes the size of the laser beam and thus limits the number
344 neurons activated (Fig. 5). In this configuration, only EPSPs but no spikes were evoked
345 in the LGMD by optogenetic stimulation. However, a cell-type specific pattern of neural
346 activation could not be achieved with currently available tools. In genetic model systems
347 such as mice and fruit flies there are ways to generate cell-type specific gene expression.
348 In mice, for example, the Cre-LoxP system drives cell-type specific expression through
349 defined promoters (Sauer, 1998). In flies, the Gal4-UAS binary system mentioned above
350 achieves the same goal (Busson and Pret, 2007). For transient gene expression in locusts,
351 it would also be desirable to target genes to specific cell types. However, this is not yet
352 feasible due to lack of identification of cell-type specific promoters and of transgenic
353 locust lines expressing an effector gene under their control.
354
355 Yet, other possibilities to target gene expression in specific cell types exist. Micro RNAs
356 (miRNAs) are small noncoding RNAs involved in posttranscriptional regulation of gene
357 expression (Obernosterer et al., 2006). Recently, miRNAs have been applied to de-target
358 gene expression when using a SFV-derived oncolytic virus to treat tumors such as
359 glioblastoma (Ramachandran et al., 2017; Ylösmäki et al., 2013). The working principle
360 of miRNAs is that by integrating the complementary sequence of a miRNA in the viral
361 genome downstream of the viral subgenomic promoter, the miRNAs expressed in
362 specific cells can identify the complementary sequence and cause the degradation of viral
363 mRNA. This in turn reduces the expression of viral proteins in those cells. Wild-type
364 SFV is naturally neurotropic (e.g., Ehrengruber et al., 1999). So, to protect neurons from

365 SFV based cancer virotherapy, the neuron-specific miRNAs, miR124, miR125, and
366 miR134 were inserted into the SFV4 vector genome. This resulted in attenuated neuro-
367 virulence in cultured neurons, astrocytes, and oligodendrocytes, and it also attenuated
368 neurovirulence in adult mice, but the modified virus retained its replication ability in
369 murine neural stem cells where the expression of these miRNAs is low (Ramachandran et
370 al., 2017; Ylösmäki et al., 2013).
371
372 Interestingly, abundant miRNAs have been identified in tissues of a species closely
373 related to that studied here, *Locusta migratoria*, including the pronotum, testes, antennae,
374 fat bodies, and brains (Wang et al., 2015). Homology searches indicated that tissue-
375 specific miRNAs were also lineage-specific and that many of them were specifically
376 expressed in the brain. Thus, provided information becomes available in the future on the
377 expression pattern of the miRNAs in specific cell populations, such as excitatory or
378 inhibitory neurons, one could add their complementary sequence to SFV plasmids and
379 obtain specific gene expression in the locust.
380
381 Injecting a viral vector containing a gene of interest in insects will only produce transient
382 expression. Creating a transgenic line would be optimal to get stable foreign gene
383 expression. Although there are no reported transgenic locusts, transgenic houseflies
384 (Hediger et al., 2001), silkworms (Tamura et al., 2000), ants (Trible et al., 2017),
385 honeybees (Schulte et al., 2014), and crickets (Nakamura et al., 2010) have been created
386 using a transposon *piggyBac*-derived vector. In the locust, one recently identified miRNA
387 precursor is likely a transposable element (TE) from a long-interspersed element family
388 (Wang et al., 2015). One could thus try this putative locust specific transposable element
389 or use the transposon *piggyBac*-derived vector described by Nakamura et al. (2010) to
390 generate germ transformation.
391
392 **Acknowledgements**
393 We thank Dr. Hiromu Yawo and Dr. Toru Ishizuka for providing pChopWR-Venus. We
394 also thank Dr. Emma Victoria Jones and Dr. Keith Murai for providing the plasmids
395 pENTR2B and pScaA7-RFA, and Dr. Alan L. Goldin for pSFV-Helper2.

Grants

This work was supported by a grant from the NIH (MH-065339) and the NSF (IIS-1607518).

Disclosures

The authors declare no competing financial interests.

References

Adamantidis, A.R., Zhang, F., Aravanis, A.M., Deisseroth, K., and de Lecea, L. (2007). Neural substrates of awakening probed with optogenetic control of hypocretin neurons. Nature *450*, 420–424.

Akerboom, J., Chen, T.-W., Wardill, T.J., Tian, L., Marvin, J.S., Mutlu, S., Calderon, N.C., Esposti, F., Borghuis, B.G., Sun, X.R., et al. (2012). Optimization of a GCaMP Calcium Indicator for Neural Activity Imaging. Journal of Neuroscience *32*, 13819–13840.

Arenkiel, B.R., Peca, J., Davison, I.G., Feliciano, C., Deisseroth, K., Augustine, G.J., Ehlers, M.D., and Feng, G. (2007). In Vivo Light-Induced Activation of Neural Circuitry in Transgenic Mice Expressing Channelrhodopsin-2. Neuron *54*, 205–218.

Arrenberg, A.B., Del Bene, F., and Baier, H. (2009). Optical control of zebrafish behavior with halorhodopsin. Proceedings of the National Academy of Sciences *106*, 17968–17973.

Asakawa, K., and Kawakami, K. (2008). Targeted gene expression by the Gal4-UAS system in zebrafish. Development, Growth & Differentiation *50*, 391–399.

Bi, A., Cui, J., Ma, Y.-P., Olshevskaya, E., Pu, M., Dizhoor, A.M., and Pan, Z.-H. (2006). Ectopic Expression of a Microbial-Type Rhodopsin Restores Visual Responses in Mice with Photoreceptor Degeneration. Neuron *50*, 23–33.

Boyden, E.S., Zhang, F., Bamberg, E., Nagel, G., and Deisseroth, K. (2005). Millisecond-timescale, genetically targeted optical control of neural activity. Nature Neuroscience *8*, 1263–1268.

Brand, A.H., and Perrimon, N. (1993). Targeted gene expression as a means of altering cell fates and generating dominant phenotypes. Development *118*, 401–415.

Busson, D., and Pret, A.-M. (2007). GAL4/UAS Targeted Gene Expression for Studying Drosophila Hedgehog Signaling. In Hedgehog Signaling Protocols, (Totowa, NJ: Humana Press), pp. 161–201.

430 Cotmore, S.F., Agbandje-McKenna, M., Chiorini, J.A., Mukha, D.V., Pintel, D.J., Qiu, J.,
431 Soderlund-Venermo, M., Tattersall, P., Tijssen, P., Gatherer, D., et al. (2014). The
432 family <Emphasis Type="Italic">Parvoviridae</Emphasis>. Arch Virol *159*, 1239–
433 1247.

434 Dewell, R.B., and Gabbiani, F. (2018). Biophysics of object segmentation in a
435 collision-detecting neuron. ELife *7*, e34238.

436 DiCiommo, D.P., and Bremner, R. (1998). Rapid, High Level Protein Production Using
437 DNA-based Semliki Forest Virus Vectors. Journal of Biological Chemistry *273*,
438 18060–18066.

439 Egelhaaf, M. (2008). Fly vision: neural mechanisms of motion computation. Curr.
440 Biol. *18*, R339-341.

441 Ehrengruber, M.U., Lundstrom, K., Schweitzer, C., Heuss, C., Schlesinger, S., and
442 Gähwiler, B.H. (1999). Recombinant Semliki Forest virus and Sindbis virus
443 efficiently infect neurons in hippocampal slice cultures. Proc. Natl. Acad. Sci. U.S.A.
444 *96*, 7041–7046.

445 Ehrengruber, M.U., Renggli, M., Raineteau, O., Hennou, S., Vähä-Koskela, M.J.V.,
446 Hinkkanen, A.E., and Lundstrom, K. (2003). Semliki Forest virus A7(74) transduces
447 hippocampal neurons and glial cells in a temperature-dependent dual manner. J.
448 Neurovirol. *9*, 16–28.

449 Ehrengruber, M.U., Schlesinger, S., and Lundstrom, K. (2011). Alphaviruses: Semliki
450 Forest Virus and Sindbis Virus Vectors for Gene Transfer into Neurons. Current
451 Protocols in Neuroscience *57*, 4.22.1-4.22.27.

452 Evangelista, C., Kraft, P., Dacke, M., Labhart, T., and Srinivasan, M.V. (2014).
453 Honeybee navigation: critically examining the role of the polarization compass.
454 Philos. Trans. R. Soc. Lond., B, Biol. Sci. *369*, 20130037.

455 Fotowat, H., and Gabbiani, F. (2011). Collision Detection as a Model for Sensory-
456 Motor Integration. Annual Review of Neuroscience *34*, 1–19.

457 Gabbiani, F., Krapp, H.G., Koch, C., and Laurent, G. (2002). Multiplicative computation
458 in a visual neuron sensitive to looming. Nature *420*, 320–324.

459 Göpfert, M.C., and Hennig, R.M. (2016). Hearing in Insects. Annual Review of
460 Entomology *61*, 257–276.

461 Gradinaru, V., Mogri, M., Thompson, K.R., Henderson, J.M., and Deisseroth, K. (2009).
462 Optical Deconstruction of Parkinsonian Neural Circuitry. Science *324*, 354–359.

463 Gupta, N., and Stopfer, M. (2011). Insect olfactory coding and memory at multiple
464 timescales. Current Opinion in Neurobiology *21*, 768–773.

465 Hales, K.G., Korey, C.A., Larracuente, A.M., and Roberts, D.M. (2015). Genetics on the
466 Fly: A Primer on the Drosophila Model System. Genetics *201*, 815–842.

467 Hediger, M., Niessen, M., Wimmer, E.A., Dübendorfer, A., and Bopp, D. (2001).
468 Genetic transformation of the housefly Musca domestica with the lepidopteran
469 derived transposon piggyBac: Genetic transformation in Musca. Insect Molecular
470 Biology *10*, 113–119.

471 Imamura, M., Nakai, J., Inoue, S., Quan, G.X., Kanda, T., and Tamura, T. (2003).
472 Targeted Gene Expression Using the GAL4/UAS System in the Silkworm Bombyx
473 mori. Genetics *165*, 1329–1340.

474 Ishizuka, T., Kakuda, M., Araki, R., and Yawo, H. (2006). Kinetic evaluation of
475 photosensitivity in genetically engineered neurons expressing green algae light-
476 gated channels. Neuroscience Research *54*, 85–94.

477 Lewis, D.L., DeCamillis, M.A., Brunetti, C.R., Halder, G., Kassner, V.A., Selegue, J.E.,
478 Higgs, S., and Carroll, S.B. (1999). Ectopic gene expression and homeotic
479 transformations in arthropods using recombinant Sindbis viruses. Curr. Biol. *9*,
480 1279–1287.

481 Lin, J.Y. (2011). A User's Guide to Channelrhodopsin Variants: Features, Limitations
482 and Future Developments. Exp Physiol *96*, 19–25.

483 Lundstrom, K., Abenavoli, A., Malgaroli, A., and Ehrengruber, M.U. (2003). Novel
484 semliki forest virus vectors with reduced cytotoxicity and temperature sensitivity
485 for long-term enhancement of transgene expression. Molecular Therapy *7*, 202–209.

486 Lwande, O.W., Lutomiah, J., Obanda, V., Gakuya, F., Mutisya, J., Mulwa, F., Michuki, G.,
487 Chepkorir, E., Fischer, A., Venter, M., et al. (2013). Isolation of Tick and Mosquito-
488 Borne Arboviruses from Ticks Sampled from Livestock and Wild Animal Hosts in
489 Ijara District, Kenya. Vector-Borne and Zoonotic Diseases *13*, 637–642.

490 Nagel, G., Szellas, T., Huhn, W., Kateriya, S., Adeishvili, N., Berthold, P., Ollig, D.,
491 Hegemann, P., and Bamberg, E. (2003). Channelrhodopsin-2, a directly light-gated
492 cation-selective membrane channel. Proceedings of the National Academy of
493 Sciences *100*, 13940–13945.

494 Nakamura, T., Yoshizaki, M., Ogawa, S., Okamoto, H., Shinmyo, Y., Bando, T., Ohuchi,
495 H., Noji, S., and Mito, T. (2010). Imaging of Transgenic Cricket Embryos Reveals Cell
496 Movements Consistent with a Syncytial Patterning Mechanism. Current Biology *20*,
497 1641–1647.

498 Obernosterer, G., Leuschner, P.J.F., Alenius, M., and Martinez, J. (2006). Post-
499 transcriptional regulation of microRNA expression. RNA *12*, 1161–1167.

500 Oppenheimer, D.I., MacNicol, A.M., and Patel, N.H. (1999). Functional conservation of
501 the wingless-engrailed interaction as shown by a widely applicable baculovirus
502 misexpression system. Curr. Biol. *9*, 1288–1296.

503 O'Shea, M., and Williams, J.L.D. (1974). The anatomy and output connection of a
504 locust visual interneurone; the lobular giant movement detector (LGMD) neurone.
505 Journal of Comparative Physiology A: Neuroethology, Sensory, Neural, and
506 Behavioral Physiology *91*, 257–266.

507 Ramachandran, M., Yu, D., Dyczynski, M., Baskaran, S., Zhang, L., Lulla, A., Lulla, V.,
508 Saul, S., Nelander, S., Dimberg, A., et al. (2017). Safe and Effective Treatment of
509 Experimental Neuroblastoma and Glioblastoma Using Systemically Delivered Triple
510 MicroRNA-Detargeted Oncolytic Semliki Forest Virus. Clinical Cancer Research *23*,
511 1519–1530.

512 Sauer, B. (1998). Inducible Gene Targeting in Mice Using the Cre/loxSystem.
513 Methods *14*, 381–392.

514 Schulte, C., Theilenberg, E., Müller-Borg, M., Gempe, T., and Beye, M. (2014). Highly
515 efficient integration and expression of piggyBac-derived cassettes in the honeybee
516 (Apis mellifera). Proc. Natl. Acad. Sci. U.S.A. *111*, 9003–9008.

517 Segev, E., Reimer, J., Moreaux, L.C., Fowler, T.M., Chi, D., Sacher, W.D., Lo, M.,
518 Deisseroth, K., Tolias, A.S., Faraon, A., et al. (2016). Patterned photostimulation via
519 visible-wavelength photonic probes for deep brain optogenetics. Neurophotonics *4*,
520 011002.

521 Spindler, S.R., and Hartenstein, V. (2010). The Drosophila neural lineages: a model
522 system to study brain development and circuitry. Dev. Genes Evol. *220*, 1–10.

523 Srinivasan, M.V. (2010). Honey bees as a model for vision, perception, and cognition.
524 Annu. Rev. Entomol. *55*, 267–284.

525 Strauss, J.H., and Strauss, E.G. (1994). The alphaviruses: gene expression, replication,
526 and evolution. Microbiol. Rev. *58*, 491–562.

527 Tamura, T., Thibert, C., Royer, C., Kanda, T., Eappen, A., Kamba, M., Kômoto, N.,
528 Thomas, J.-L., Mauchamp, B., Chavancy, G., et al. (2000). Germline transformation of
529 the silkworm Bombyx mori L. using a piggyBac transposon-derived vector. Nature
530 Biotechnology *18*, 81–84.

531 Trible, W., Olivos-Cisneros, L., McKenzie, S.K., Saragosti, J., Chang, N.-C., Matthews,
532 B.J., Oxley, P.R., and Kronauer, D.J.C. (2017). orco Mutagenesis Causes Loss of
533 Antennal Lobe Glomeruli and Impaired Social Behavior in Ants. Cell *170*, 727-
534 735.e10.

535 Wang, H., Sugiyama, Y., Hikima, T., Sugano, E., Tomita, H., Takahashi, T., Ishizuka, T.,
536 and Yawo, H. (2009). Molecular determinants differentiating photocurrent
537 properties of two channelrhodopsins from chlamydomonas. J. Biol. Chem. *284*,
538 5685–5696.

539 Wang, Y., Jiang, F., Wang, H., Song, T., Wei, Y., Yang, M., Zhang, J., and Kang, L. (2015).
540 Evidence for the expression of abundant microRNAs in the locust genome. Scientific
541 Reports *5*, 13608.

542 Wehner, R. (2003). Desert ant navigation: how miniature brains solve complex
543 tasks. J Comp Physiol A *189*, 579–588.

544 Wimmer, V.C., Nevian, T., and Kuner, T. (2004). Targeted in vivo expression of
545 proteins in the calyx of Held. Pflugers Arch - Eur J Physiol *449*, 319–333.

546 Ylösmäki, E., Martikainen, M., Hinkkanen, A., and Saksela, K. (2013). Attenuation of
547 Semliki Forest Virus Neurovirulence by MicroRNA-Mediated Detargeting. J. Virol. *87*,
548 335–344.

549

550

551 **Figure Legends**

552

553 **Figure 1.** Semliki Forest Virus (SFV) drives Chop-wide receiver (ChopWR)-Venus
554 expression in medullary neurons of the locust optic lobe. **A**, Schematic diagram showing
555 the plasmid used to generate the SFV A7(74) based vectors encoding ChopWR-Venus.
556 The viral backbone is derived from pSFV(A774nsP) (Ehrengruber, et al. 2003). **B**, a),
557 Medullary neurons somata expressed ChopWR-Venus in the locust optic lobe (white
558 arrows). b), Bundles of transmedullary axons expressing ChopWR-Venus (white arrow)
559 travel towards the lobula neuropil (grey arrow). c) and d), Double stain of the LGMD
560 excitatory dendritic field (Alexa 594, red) and Venus-labeled transmedullary neuron
561 terminal arbors (green) show close apposition in the lobula. Abbreviations, *L*: lateral, *M*:
562 medial, *D*: dorsal, *V*: ventral. Scale bars are listed in each panel.

563

564 **Figure 2.** Laser stimulation via optic fiber with a diameter of 200 μm activated the
565 medullary neurons (Med) expressing ChopWR-Venus and the LGMD. **A,** The
566 instantaneous firing rate of the medullary neurons expressing ChopWR-Venus was
567 increased during 5 s of 488 nm laser stimulation; top, laser stimulation timing; bottom,
568 blue trace is the averaged firing rate across 4 trials (light blue traces). Rasters below the
569 IFR show the medullary neuronal spikes. **B**, The mean firing rate of the medullary
570 neurons expressing ChopWR-Venus across 6 locusts (red dots) was compared with and
571 without laser stimulation; * indicates p = 0.0156 (one-sided WSRT). **C,** The
572 instantaneous firing rate of the LGMD increased during 5 s of 488 nm laser stimulation;
573 green trace is the averaged firing rate across 4 trials (light green traces). Rasters below
574 the IFR show the LGMD spikes. **D**, The mean firing rate of the LGMD across 6 locusts
575 (red dots) was compared with and without laser stimulation; * indicates p = 0.0156. **E**,

The LGMD V_m was depolarized during 5 s of 488 nm laser stimulation in a ChopWR-expressing locust (top), while no depolarization was observed in an un-transfected control (bottom). Black trace represents the averaged V_m and gray traces are individual trials (4 trials in the ChopWR-expressing locust and 6 trials in the wild type locust). **F**, Plot of the mean median LGMD V_m (± 1 s.d.) with and without laser stimulation in 6 animals. * indicates p = 0.0156.

Figure 3. Laser stimulation triggers inhibitory inputs to the LGMD that can be blocked by the $GABA_A$ receptor antagonist picrotoxin (PTX). **A**, Laser stimulation (2 s, 488 nm) via an optic fiber with diameter of 10 μm triggered the firing of the LGMD. Top, laser stimulation timing; middle, the LGMD V_m from 1 trial; bottom, the averaged LGMD IFR (gray trace) across 5 trials (light gray traces). The rasters below are the spikes of the LGMD from 5 trials. **B**, Puffing PTX increased laser-triggered firing in the LGMD. Top, laser stimulation timing; middle, the LGMD V_m from 1 trial; bottom, the averaged LGMD IFR (gray trace) across 5 trials (light gray traces). The rasters below are the spikes of the LGMD from 5 trials. **C**, The mean firing rate of the LGMD triggered by laser stimulation was compared with and without puffing PTX. **D** and **E**, mean firing rate of the LGMD triggered by laser onset (D) and offset (E) were compared with and without puffing PTX. Red symbols indicated the mean values across 3 locusts.

Figure 4. The firing of the LGMD increased and saturated in response to increasing laser power. **A**, Examples of the LGMD IFR in response to laser powers of 2, 8 and 16 mW (from top to bottom; one locust). Laser stimulation timing is shown above the top panel (duration: 5 s). Each panel shows the averaged LGMD IFR (dark purple) from 5 trials (light purple). The rasters below the LGMD IFR are the LGMD spikes from the 5 trials (p = 0.0312 and 0.125 between groups with laser power at 2 vs. 8 and 8 vs. 16 mW by a one-sided WSRT). **B**, The number of LGMD spike evoked by laser stimulation increased and saturated with increasing power. Blue circles indicate the mean value in each group. A Kruskal-Wallis test was used to evaluate the effect of laser power across groups (p=0.013). A post-hoc signed rank test was used to evaluate the difference between two groups (p values on panel; ns, no significant difference).

Figure 5. A laser probe narrowing the region activated by the laser elicited only EPSPs in the LGMD. **A**, Schematics of the laser probe (left) and optic fiber (right). Dashed lines indicate light path. In the laser probe, the beam exits perpendicular to the shaft thanks to a mirror. **B**, Laser probe stimulation (5 s, 488 nm) triggered EPSPs in the LGMD. Top, laser stimulation timing; bottom, the averaged LGMD V_m (black trace) across 4 trials (gray traces). **C**, Comparison of the mean across 3-5 trials of the LGMD V_m (± 1 s.d.) for 5 locusts with and without laser stimulation. For each animal the mean V_m was higher during the laser stimulation and higher during the first 2 s than the last 3 s of laser stimulation. * indicates p = 0.0312 by a one-sided WSRT.

A

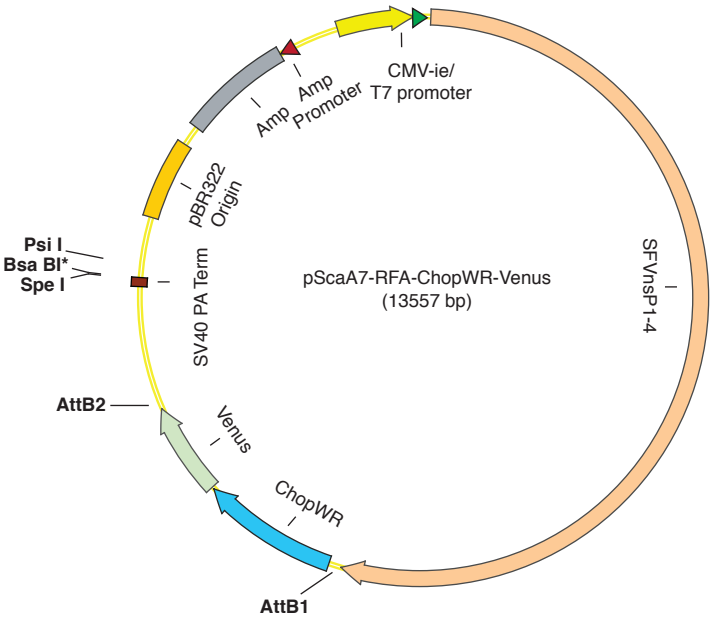

B

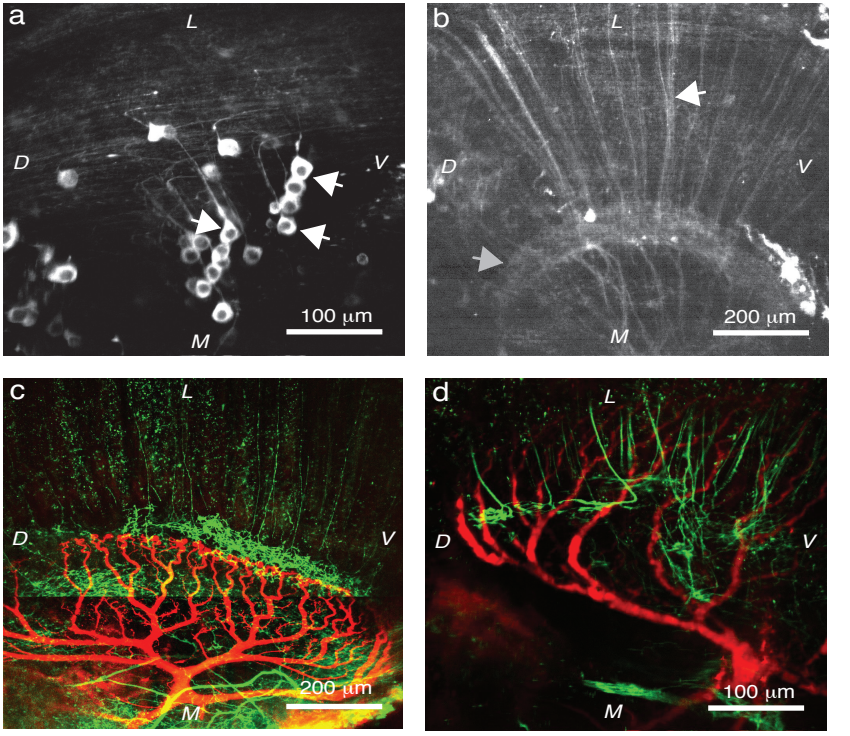

Wang et al., Fig. 1

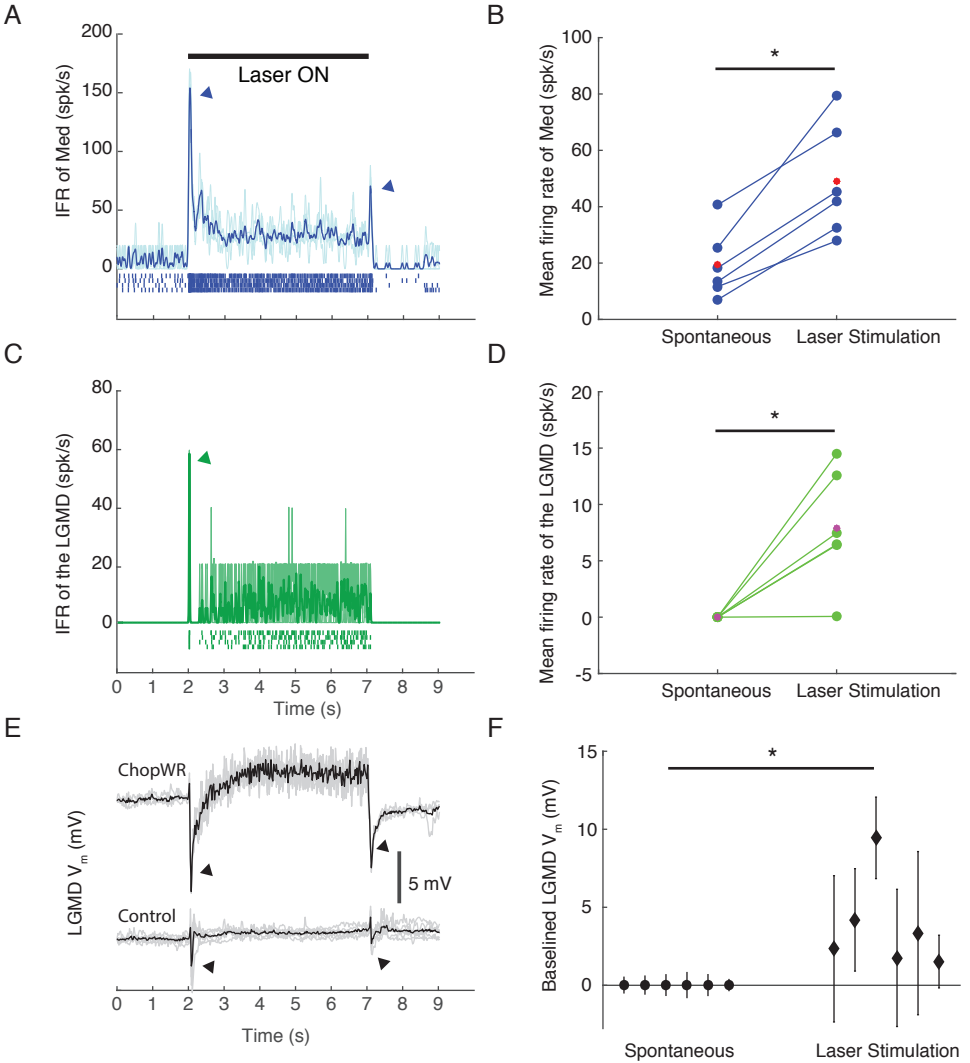

Wang et al., Fig. 2

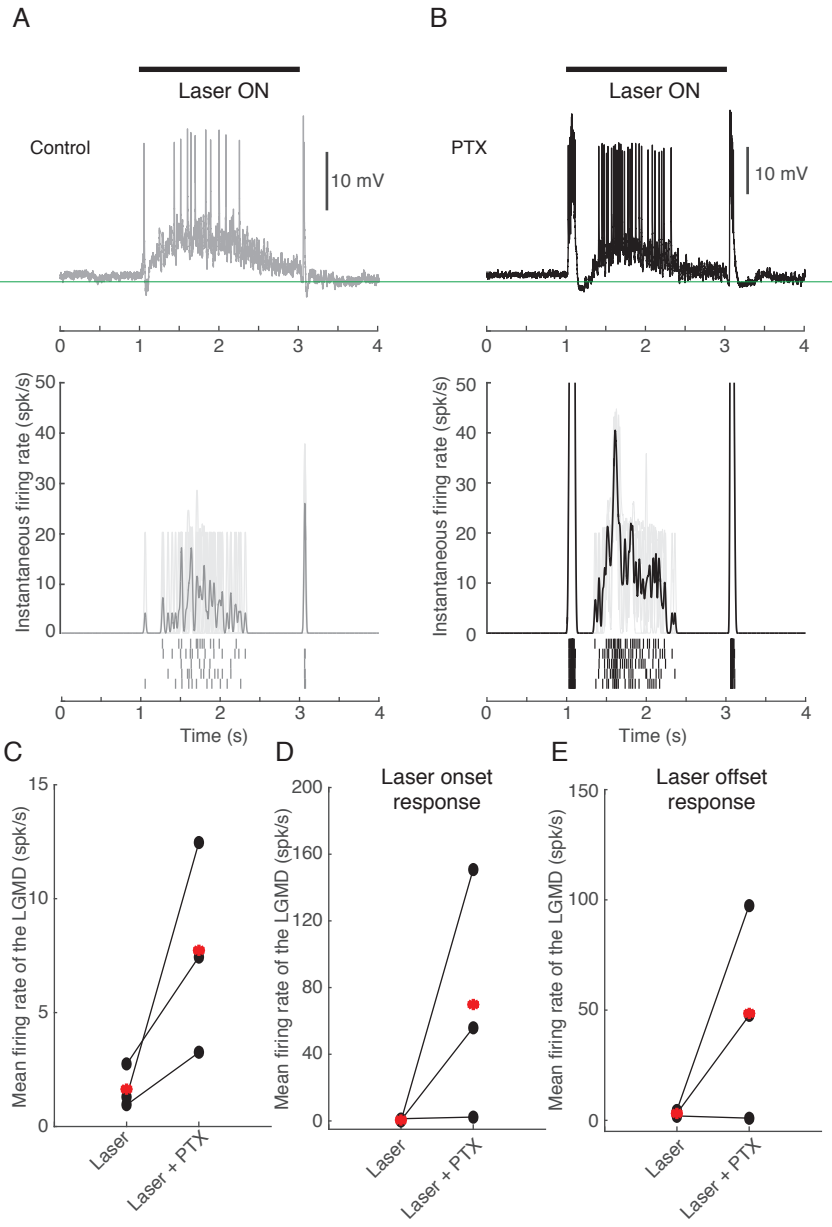

Wang et al., Fig. 3

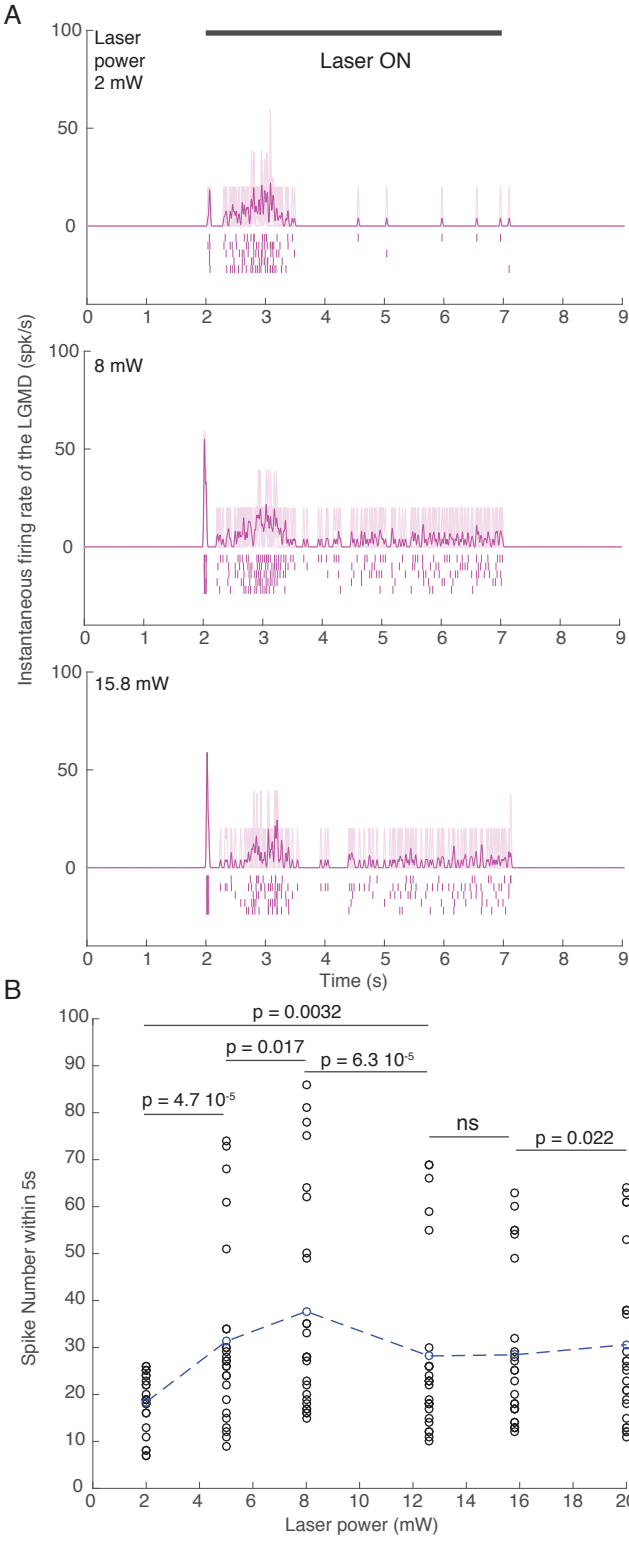

Wang et al., Fig. 4

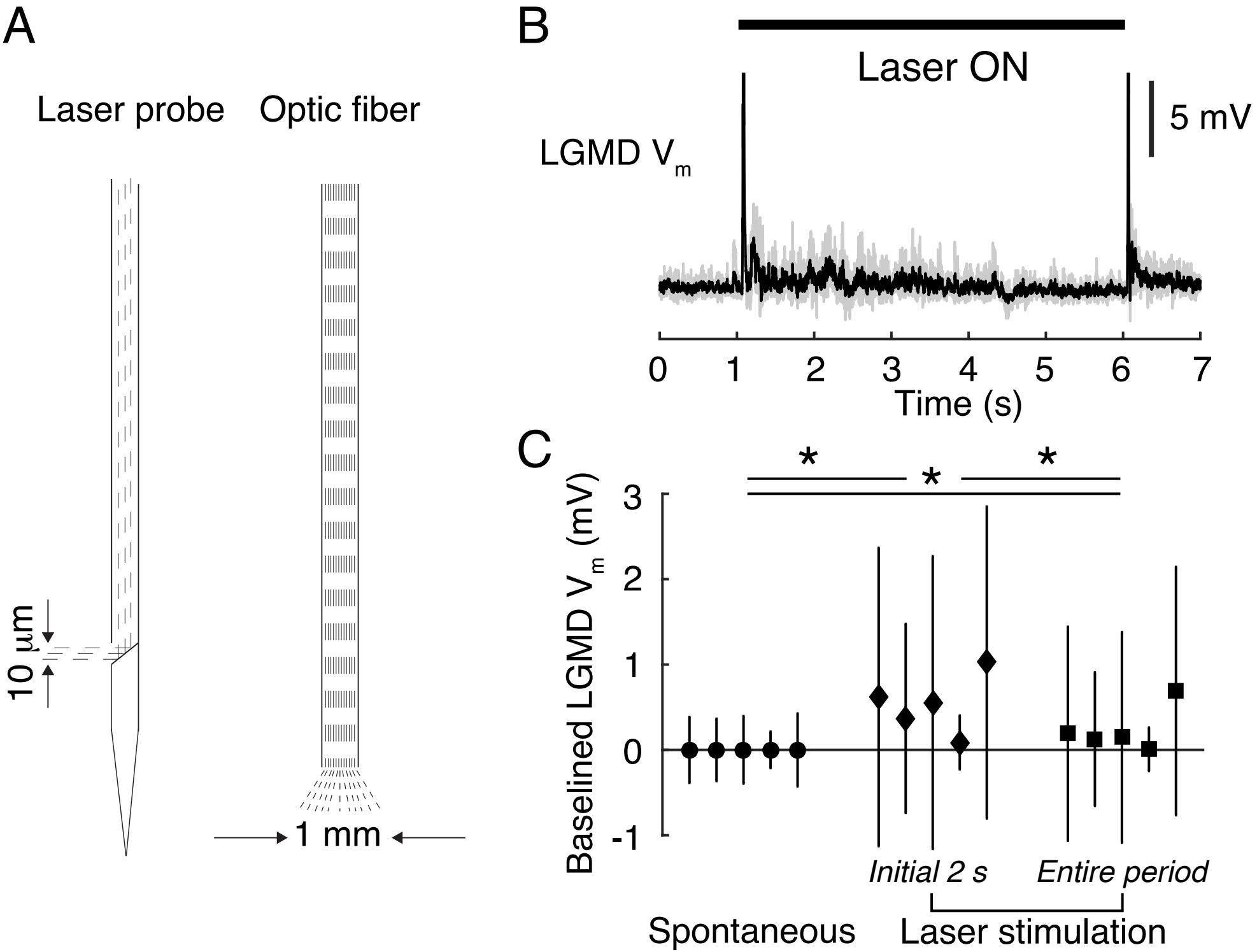

Wang et al., Fig. 5